INTERNATIONAL JOURNAL of RENEWABLE ENERGY RESEARCH
H. Sadig et al., Vol.15, No.4, December, 2025

Characterization and Kinetic Study of Saudi Arabian Olive Wastes for Thermochemical Conversion

Hussain Sadig*‡, Abdul Haleem E. Al-Rahmoun*, Abdullah O. Al-Mutawa*, Thamer D. Al-Mutairi*, Abdullah Alghafis*, Mohamed Nejlaoui*

* Department of Mechanical Engineering, College of Engineering, Qassim University, Unaizah, Saudi Arabia

(H.SADIG@qu.edu.sa, 361118069@qu.edu.sa, 352115802@qu.edu.sa, 352108801@qu.edu.sa, a.alghafis@qu.edu.sa, m.nejlaoui@qu.edu.sa)

‡Corresponding Author; Hussain Sadig, Department of Mechanical Engineering, College of Engineering, Qassim University, Unaizah, Saudi Arabia Tel: +966532629117, H.SADIG@qu.edu.sa

Received: 13.12.2023 Accepted:23.01.2024

Abstract- Olive oil industry in the northern of Saudi Arabia generates huge amount of wastes which would affect on environment if not properly disposed. In this work, the suitability of olive wastes for thermochemical conversion was studied experimentally. The study includes an investigation of the physical, combustion, elemental and kinetic characteristics of olive wastes. Three samples from Domat Al-Jandal-KSA (29°48′41″N 39°52′06″E) and Elgrayat-KSA (31°19′N 037°22′E) were collected and investigated experimentally. For kinetic investigation, Kissinger and the distributed activation energy model (DAEM) were implemented where 5, 10, 30, 50 K/Min heating rates were used. The lower calorific value for Domat Al-Jandal samples was found to be 24152.5.2kJ/kg while for Elgrayat samples were found to be 13386kJ/kg and 12568.5kJ/kg, respectively. The elemental investigation for the samples showed higher carbon and hydrogen content for Domat Al-Jandal sample with 50% and 8%, respectively. Based on Kissinger model the activation energy for Domat Al-Jandal sample were found to be 168.502kJ/mol while for Elgrayat samples it was ranging from 122.755 to 135.736kJ/mol. On the other hand, the pre-exponential factor values were within the range of of 1.125×10^3 to3.954×10^{13}. In general, the collected results showed that Domat Al-Jandal olive wastes have a higher potential to undergo thermochemical conversion as compared with Elgrayat wastes.

Keywords Biomass energy, olive wastes, TGA, kinetic study, thermochemical conversion.

1. Introduction

With the increase of global awareness on energy problems, renewed attention was given to use of biomass wastes as a promising resources [1, 2]. Olive plantation and olive oil industry is a key economical, industrial and social factor in many countries such as Mediterranean countries [1, 3, 4]. The northern regions of the kingdom of Saudi Arabia (KSA) are known with olive industry where most of available lands were used for olive cultivation [5-9]. The growing interest in cultivation of olive by private sector was affected in increasing of the production olive oil in the country where the production of olive oil was 3000 MT in 2013 [10]. Generally, the production process of olive oil from olive fruits is associated with huge amounts of wastes that would affect negatively on environment unless it disposed properly [1, 3, 4, 7, 11-13].

Biomass can be converted into useful fuel by implementation of different techniques including biochemical and thermochemical techniques [14-19]. Thermochemical energy conversion is a suitable way to convert solid biomass wastes into different types of fuels including solid, liquid and gas fuels[4, 15, 20-22]. In addition, thermochemical energy conversion processes provide many advantages including volume and mass reduction of the disposed biomass materials, reduction of pollutants and its high energy recovery potential [15, 20, 23, 24]. The utilization of these wastes in energy production would affect positively on the environmental and enhances the sustainable use of the limited energy resources [3, 7]. Although the availability of huge amounts of olive wastes which resulted from olive industry in this regions no studies were conducted to utilize these wastes for energy production. Since Saudi 2030 vision is looking forward to use of various energy resources including energy from biomass. The implementation of such wastes for power production would reduce the country reliance on fossil fuels.

Numerous studies on the characterization of olive wastes were conducted previously. Gogu and Maskan [25] studied

experimentally the drying behavior of olive pomace at different temperature, sample thickness and different particle size. The study showed a considerable improvement in the drying time for olive pomace by implementing of different sample thickness. on the other hand, the study proofed that the olive pomace drying process is strongly affected by the drying air temperature and olive pomace particle size.

Roberto Volpe et al. [13] conducted an experimental investigation on the elemental characteristics and mass reduction behaviour of different types of olive wastes including Olive pulp and olive tree trimmings. The study showed that at a temperature of 650oC, the reduction in sample weight was up to 74% of its masses. In addition, the analyses of chars showed a direct increase of carbon percentage up to values of 75% and a reduction of oxygen percentage up to values of 10%. On the other hand, the H-content remained stable up to a temperature of 300oC and then decreased with the increase of peak temperature.

In order to find the best blend option, Miranda et al. [26] studied the combustion and characterization of olive wastes and residue from forest. In this research work, the characteristics of pelletized blends of olive residues and oak residues were investigated experimentally. Different pellets samples were produced and a stove combustion tests were used to study and investigate the combustion emissions of each sample. The results proved that not all tested samples were within quite satisfactorily levels, which was due to the different conditions of the precursors. The investigation recommended using of less than 50% of olive residues in the biomass pellets.

Alkhamis and Kablan [11] studied the potential of low cost olive cake for energy production and its impact on environment. The study was concentrated on finding of olive oil wastes calorific value and the effect of olive cake grain size on its caloric value. In addition, a process for the selection of a suitable olive cake grain size for handling, packaging and storing was proposed. The study proved that olive cake is a quite suitable for energy production with a maximum calorific value of 29.65kJ/kg when the olive waste percentage was 28.08%.

Alrawashdeh et al. [27] studied experimentally the degradation of olive residue by TGA. In this work, the investigation was focusing on the behavior of olive residuals during thermal decomposition process. The experimental work was concentrated on three different waste olive residuals including olive pomace, olive pruning and olive kernels. The samples were investigated under a nitrogen atmosphere at different heating rates, using a thermogarvimetric balance. In the experimental work, the samples were heated to a maximum temperature of 1,023 K, with four different heating rates of 2, 5, 10, 15 K/min. The kinetic data obtained from this investigation would provide useful information on the pyrolysis process which would be helpful in predicting the kinetic model.

Another study on using of tests TGA for examining the effect of pressure and beak temperature on biochar yield during pyrolysis of two-phase olive mill wastes were conducted by Manyà et al. [28]. In this work, pyrolysis investigations were conducted in a thermogarvimetric analyzer TGA under nitrogen atmosphere and at a constant heating rate of 5K/min. The collected results on yielded biochar, yielded fixed-carbon, and the temperature at which the maximum rate of weight loss is reached were analyzed using regression models. The study showed that the amount of yielded biochar from the process decreases when both peak temperature and pressure increases.

Guida et al. [12] conducted a thermogarvimetric analysis for different types of olive wastes. The studied wastes include olive mill solid waste (OMSW) and concentrated olive mill waste water (COMWW). In this study, the thermal behavior of the tested material was examined at different heating rates ranging from 5 to 50 C/min in inert atmosphere using the technique of thermogarvimetric analysis. For different increment of heating rates, the variations of characteristic parameters from the TG-DTG curves were determined. The initial temperature of degradation was higher in OMSW, which present a high amount of cellulose in comparison with COMWW. The results showed that the apparent activation energy obtained for the material derived from OMSW was in the range of 150–176 and 210.5–235.7 kJ/mol while for COMWW the values were found to be 133–145 and 255–275 kJ/mol, respectively.

Soria-Verdugo et al. [29] studied the effect of the number heating rates curves used in TGA on the study of biomass pyrolysis process. The investigation was implemented by using of the distributed activation energy model (DAEM). In this work, different biomass materials were used in the biomass characterization process including pine wood, olive kernel, thistle flower and corncob. In addition, for all biomass materials studied, nine heating rates curves were applied. The study proved a considerable reduction on the uncertainties of the collected results when increasing of the number of implemented heating rates.

In this work, the Saudi Arabian olive wastes from different location were collected and investigated. The study includes an investigation of physical, combustion and elemental properties of the olive wastes. In addition, a kinetic study on olive wastes was performed where the activation energy and per-exponential factor for different olive wastes samples were evaluated by using of two different models including Kissinger and the Distributed Activation Energy Model (DAEM). The collected results from this study would give sufficient information on the suitability of utilizing Saudi Arabian olive wastes for thermochemical conversion. Moreover, the results would help in selecting the most appropriate conversation method to be implemented to such materials and also in the design of pyrolytic equipment which relay totally on kinetic parameters of biomass material such as activation energy and thermal decomposition rates.

2. Material and Methods

2.1. Material Collection and Preparation

In this work, three different air dried olive cake waste samples were obtained from different olive oil mills located in Domat Al-Jandal-KSA (29°48′41″N 39°52′06″E) and Elgrayat-KSA (31°19′N 037°22′E). Each sample was

numbered and given specific code for preparation and sorting process. The first sample was with square cross-section was obtained from Al-Jawf region, Domat Al-Jandal governorate KSA. Another two samples with a cylindrical shape were collected from an olive farm in the Al-Jawf region, Elgrayat governorate-KSA. The first sample was given a reference code of A while the other two samples were given reference codes of B and C.

In order to prepare the samples for tests, each sample was crushed with a hammer into small and medium-sized pieces as shown in Figure 1 (a). The resulted material was then transferred to a sieve shaker device which shown in Figure 1 (b) where a smaller size was obtained. The used sieve shaker device was capable to give a material sizes in the range of 20 µm to 500 µm. Shown in Figure 1 (c) is the collected material from sieve shaker.

Since the devices used in the experimental work deals with small material sizes, specific sizes were selected to be used in this work. Thus, the selected materials sizes from sieve shaker device were with a sample sizes less than 150 µm. Finally, three samples were obtained from each material including A, B and C. Shown in Figure 1 (d) is the final stage of material perpetration where the material powder was prepared and kept in bottles.

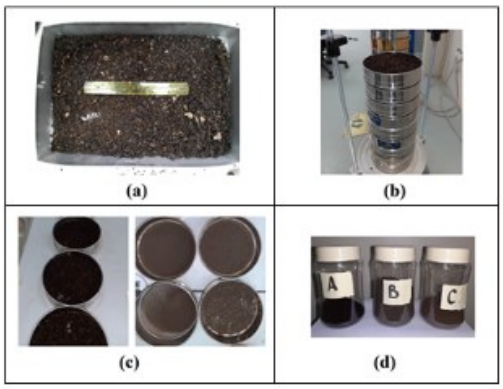

Fig. 1. (a) Samples after crushing (b) Sieve shaker device (c) Collected different sizes from sieve device (d) Final stage of material preparation.

2.2. Bulk Density Determination

The bulk densities for each sample were evaluated by using of sensitive weight and 250 mL beaker. For each sample, small amount of the prepared material was put in the beaker and the material volume and weight were measured and used to evaluate to the bulk density. For each material sample, the bulk density tests were repeated three times and the average value were taken.

2.3. Material Drying

For material drying process, small amounts of prepared samples were put in open vessels and placed into a forced air drying oven 425 litre capacity 78-00135/01/ produced by zan group at a temperature of 110 °C. The drying trends for the samples under study were obtained based on measuring of samples weight at 5 minutes time intervals. At each time interval, the material under study lost some of its weight due to water evaporation and hence lower weight is obtained till it reaches a point where there is no considerable weight lost were achieved. At this point, the samples were considered to be completely dried and the drying process was stopped.

2.4. Calorific Value Determination

The calorific value was calculated with the accordance to CEN/TS 14918. For the test purpose, a calibrated Parr 6200 bomb calorimeter was used to determine the higher and lower calorific value for the tested samples.

2.5. Ultimate Analysis

The mass percentages of carbon (C), nitrogen (N), hydrogen (H) and sulphur (S) were determined by using of a 2400 Series II CHNS/O elemental analyzer. Small amounts of the material under study typically ranging from 1.5 to 2.2 grams were investigated by using of CHN analyzer. Oxygen percentage in the samples was evaluated by subtraction.

2.6. Proximate Analysis

In order to predict the thermal behavior of any biomass material, the biomass weight loss due to temperature increase at specified time is measured. Thermogarvimetric analysis (TGA) is a commonly used technique to conduct the proximate analysis of biomass materials [30]. TGA provides an extensive understanding of biomass material thermal degradation behavior which occurs in thermochemical conversion processes. In this work, proximate analyses were carried out by using TGA Q500 model Thermogarvimetric Analyzer. Typically, 10 to 40 mg of samples was used to evaluate of moisture content, volatile matter, fixed carbon and Ash content of the material under study. In order to study the kinetic parameters of the biomass material, the thermal degradation tests TGA was conducted with at different heating rates from material's initial conditions till 1273 K. Nitrogen was used as purge gas and isothermal for 5 minutes were applied.

2.7. Kinetic Model

The de-volatilization process is considered as the first step in all thermochemical conversion processes. Based on biomass material nature, a continuous heating of biomass material would affect in splitting of biomass chemical bonds. The process is very complex, but it can be simplified into one step model which assumes that the process takes place in a single step. Reaction models are commonly used to analysis the biomass degradation behaviour where it assumes that the reaction rate is proportional to the reaction order (n).

$$\frac{d\alpha}{dT} = k(T)(1-\alpha)^n \quad (1)$$

Where $k(T)$ is the kinetic rate constant.

The kinetic rate constant can be represented based on Arrhenius equation as following:

$$k(T) = A.e^{-\frac{E_a}{RT}} \quad (2)$$

Where:

k: $Reaction\ rate\ constant\ (s^{-1})$

T: $temperature\ (K)$

A: $Pre-exponential\ factor\ (s^{-1})$

E_a: $Activation\ energy\ (^{J}/_{Kmol})$

R: $gas\ constant\ (^{J}/_{Kmol})$

In this work, the Kissinger and the Distributed Activation Energy Model (DAEM) methods were applied to obtain the kinetic parameters of the biomass material under mass degradation process. The kinetic parameters include the activation energy and pre-exponential factor for the biomass samples under study.

Kissinger model assumes that the reaction rate reaches its maximum value at (T_p) which can be represented in DTG curves. The governing equation for Kissinger model as follows:

$$\ln\left(\frac{\beta}{T_p^2}\right) = \ln\left(\frac{AR}{E_a}\right) - \frac{E_a}{RT_p} \quad (3)$$

Where:

(β): the heating rate (K/min).

T_p: Peak temperature (K)

In order to apply Kissinger method, four TGA experiments at different heating rate including 5 K/min, 10 K/min, 30 K/min and 50 K/min were conducted for the material under study including sample A, B and C. From TGA results, the DTG curves for the different heating rate were plotted and the points of T_p for each heating rate were obtained. Based on the collected data from DTG curves, Kissinger plot which represents the relation between ($\ln\left(\frac{\beta}{T_p^2}\right)$) and ($\frac{1000}{T_p}$) [31] were plotted. Finally, based on Kissinger plot, the value of activation energy and pre-exponential factor were evaluated from slope and intercept.

The Distributed Activation Energy Mode (DAEM) was first proposed by Vand [32]. DAEM assumes a number of first order reaction which follow Arrhenius kinetics equation and occur at the determined activation energy of the fuel chemical reaction. However, the proposed method was very complicated and simplified by Miura [33, 34]. In this model, the biomass de-volatilization process can be described by:

$$1 - \frac{V}{V^*} = \int_0^\infty \exp\left(-A\int_0^t e^{-E/RT}\,dt\right) f(E)\,\mathrm{dE} \quad (4)$$

Where:

V: $Volatiles\ loss\ (mg)$

V^*: $Total\ volatiles\ (mg)$

V: $Time\ (s)$

The time integral in the exponential function in Equation (4) can be converted into temperature as following:

$$\emptyset(E,T) = \exp\left(-\frac{A}{\beta}\int_0^T e^{-E/RT}\,dT\right) \quad (5)$$

Equation (5) can be further simplified to:

$$\emptyset(E,T) = \exp\left(-\frac{ART^2}{\beta E}e^{-E/RT}\right) \quad (6)$$

By implementing of Miura simplification, the Arrhenius equation can be expressed as:

$$\ln\left(\frac{\beta}{T^2}\right) = \ln\left(\frac{AR}{E}\right) + 0.6075 - \frac{E}{RT} \quad (7)$$

Based on TGA collected results for the samples under study at different heat rates, $\frac{V}{V^*}$ at the different temperatures were evaluated and plotted as de-volatilization curves at different heating rate. From Arrhenius plot which shows the relation between $\frac{\beta}{T^2}$ and $\frac{1}{T}$ at selected de-volatilization rate, the activation apparent energy Ea, and the pre-exponential factor (A) are determined from the slope and intercept.

3. Results and Discussions

3.1. Calorific Value

In this work, the lower and higher calorific value of olive wastes samples A, B and C were evaluated in bomb calorimeter. Shown in Table 1 is the variation in lower and higher calorific value of the tested samples. As it can be seen from the Table, sample A showed higher calorific values as compared with sample B and C. The lower and higher calorific values for sample A were found to be 24152.5kJ/kg and 24889.2kJ/kg, respectively. On the other hand, the corresponding values were found to be 13386.0kJ/kg and 13824.2kJ/kg for sample B and 12568.5kJ/kg and 12907.9kJ/kg for sample C. As it can be seen from the Table, sample A was higher with 44.5% to 48% as compared with other samples. This is may be due to the poor storage conditions and dust to which the samples were exposed. In addition, it was very clear that the period during which storage was carried out was affected negatively on biomass quality including calorific value since some of volatiles may lost due to poor storage conditions for long periods. As it can be seen from Table 3 the volatile contents was very high in sample A which was affected strongly in its high calorific value.

Table 1. Lower and higher calorific value for sample A, B and C

Material	LCV (kJ/kg)	HCV (kJ/kg)
Sample A	24152.5	24889.2
Sample B	13386.0	13824.2
Sample C	12568.5	12907.9

The collected results were also compared with other solid fuels including different types of solid biomass wastes and coal. Figure 2 shows a comparison of olive waste samples A, B and C calorific values with other different types of wood wastes and coal [35-37]. As can be seen from the Figure, sample A showed higher calorific values as compared to wood and some types of coal such as Bituminous coal (23250 MJ/kg) which is commonly used for the heat production in industrial and residential sectors. On the other hand, as compared to other materials, samples B, C showed lower

calorific values. In general, in term of calorific value, the collected results showed a superior value for olive residues which would enhances the capability of utilization of such wastes as a fuel.

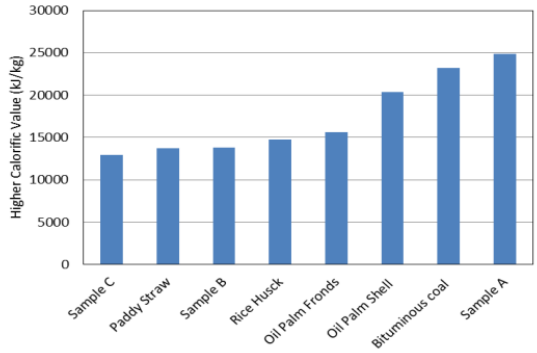

Fig. 2. Comparison of calorific value of the tested olive waste samples and different types of wood wastes and coal.

3.1. Elemental analysis

Elemental investigation is very important part in the study of suitability of any biomass material for thermochemical conversion processes. CHN analysis is a common technique for assessing the elemental and environmental compatibility of different material including fossil fuels such as coal, as well as for recycling of raw materials such as wood or biomass combustible waste. In this work, CHN analyzer was used to evaluate the mass percentages of carbon (C), nitrogen (N), hydrogen (H) and sulfur (S). Small amounts of olive waste material including A, B and C were experimentally tested in CHN analyzer.

Shows in Table 2 is the mass percentage of carbon (C), nitrogen (N), hydrogen (H) and sulfur (S) for the tested olive waste samples including A, B and C and other biomass and different type of coal [35]. As can be seen from the Table, sample A showed higher percentage of carbon and hydrogen percentages as compared with sample B and C. In addition, for all tested samples, the percentages of nitrogen and sulfur were in the same ranges, where the nitrogen and sulfur ranges were found to be in the range of 0.26% to 0.53% and 2.69% to 3.89%, respectively. In general, the collected elemental investigation results showed higher quality for olive wastes collected from Domat Al-Jandal farms as compared with Elgrayat farms since the higher percentage of carbon and hydrogen in this biomass material which would affect releasing of higher amount of heat energy during combustion.

Table 2. Mass percentage of Carbon (C), Nitrogen (N), Hydrogen (H) and Sulfur (S) for the tested olive waste samples and other materials

Material	Carbon (C) (%)	Hydrogen (H) (%)	Nitrogen (N) (%)	Sulfur (S) (%)
Sample A	50.04	7.99	0.53	3.89
Sample B	29.55	4.21	0.51	2.75
Sample C	30.06	4.17	0.26	2.69
Bituminous Coal	68.00	4.00	3.00	0.90
Oil Palm Fronds	42.10	5.46	0.70	0.13
Oil Palm Shell	49.65	6.13	0.41	0.48
Rice Husk	38.74	5.83	0.55	0.06
Paddy Straw	33.48	6.01	1.46	0.15

The results obtained were also compared with other solid fuels, including solid biomass wastes and various forms of coal. Shown in Table 3 also is a comparison of sample A with different types of woody biomass wastes and coal. As can be seen from the Table, sample A showed higher Hydrogen percentage as compared to saw dust, wheat straw, peat and coal which is advantage since the higher percentage of hydrogen would affect positively on calorific value. On the other hand, the percentage of carbon in sample A was found to be higher as compared with saw dust and wheat straw and lower as compared with peat and coal.

The percentage of sulfur in sample A was found to be higher as compared to saw dust, wheat straw, peat and coal which is disadvantage since the combustion of materials with higher sulfur percentage would results in higher sulfur oxides which is undesirable product. In general, the results obtained from elemental investigation of Saudi Arabian olive wastes showed higher opportunity to undergo into thermochemical energy conversion which gives the possibility of using this waste as fuel. Moreover, due to the harmful effect of sulfur oxides more attention should be given when using of olive wastes in the different thermochemical energy conversion processes.

3.2. Mass Degradation Behaviour

In this work, TGA analysis was conducted for the samples under study including A, B and C. The three samples were tested in a TGA analyzer under same conditions. The samples temperature was increased gradually from ambient condition till it reached a maximum temperature of 1273K where the experiment was stopped. Shown in Figures 3-5 are the mass thermal degradation behavior and derivative mass loss curve (DTG) of sample A, B and C at constant temperature increment of 5K/min. As it can be seen from the figures, a gradually mass degradation was occurred with the increase of the temperature. Based on the collected results, for the same combustion rate, different mass degradation trend was achieved and each sample has its own unique degradation behavior.

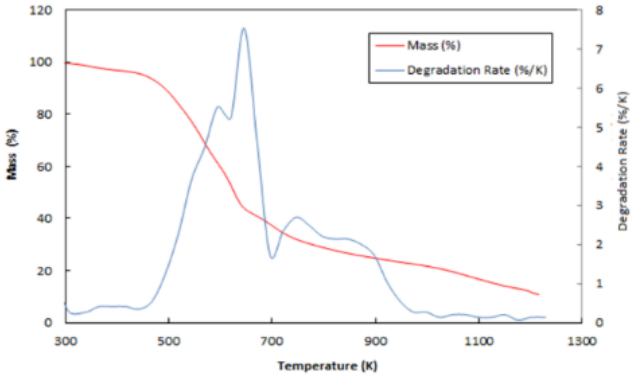

Fig. 3. The mass thermal degradation behavior and derivative mass loss curve (DTG) of sample A at heating rate of 5K/min.

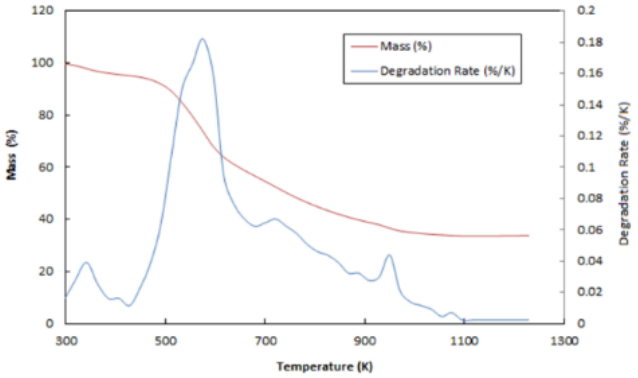

Fig. 4. The mass thermal degradation behavior and derivative mass loss curve (DTG) of sample B at heating rate of 5K/min.

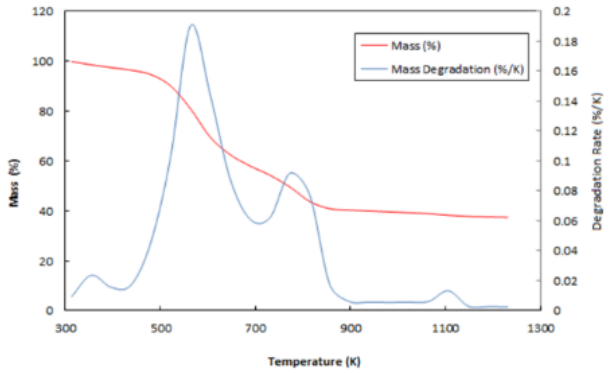

Fig. 5. The mass thermal degradation behavior and derivative mass loss curve (DTG) of sample Cat heating rate of 5K/min.

As it can be seen from the Figures, the degradation of the samples under study begins around 310K. Two main peaks can be noticed clearly in sample A degradation curve while sample B and C showed only one peak. For sample A, the first peak which was at 590K is related to the thermal degradation of hemicellulose, while the second peak at 640K is attributed to the degradation of cellulose [38]. Sample B and C showed only one peak at 580K and 570K, respectively which were attributed to degradation of hemicellulose. The sharper hemicellulose peak of sample B and C represents the higher hemicellulose percentage in sample B and C as compared with sample A. The shoulder followed the second peak is attributed to the thermal degradation of lignin which was found to be at 750K for sample A while for sample B and C was at around 720K.

In order to analysis the collected results of samples degradation trends, the mass degradation curves were divided into three temperature zones. The first zone starts from the ambient conditions till a temperature of 473K. This zone represents the water evaporation zone where the total amounts of moisture inside the samples are assumed to evaporate in this zone. The second zone which ends at temperature of 680K represents the hemicelluloses and celluloses zone, where the total amounts of volatile are assumed to burn by the end of this zone. The last zone ends at 1273K and represents the of fixed carbon zone. The personage of the ash in samples was assumed to be the remaining percentage. Based on the explained temperature zones, shown in Table 4 are the percentages of moisture, volatile, fixed carbon and ash content for samples under investigation and other different types of biomass and coal materials.

Table 3. The percentages of moisture, volatile, fixed carbon and ash content for samples under investigation and other different types of biomass and coal materials

Material	Moisture Content (%)	Volatile Contents (%)	Carbon Content (%)	Ash (%)
Sample A	4.00	72.00	16.00	8.00
Sample B	5.00	39.00	22.00	34.00
Sample C	4.00	38.00	18.00	40.00
Bituminous Coal	11.00	35.00	45.00	9.00
Oil Palm Fronds [25]	71.43	83.19	12.66	4.15
Oil Palm Shell [25]	17.50	81.03	14.52	4.44
Rice Husk [25]	13.08	64.20	12.57	23.24
Paddy Straw [25]	8.47	72.48	8.08	19.75

As it can be seen from Table 3, it is noticed that the percentage of moisture, volatile, carbon and ash content in sample A are 4%, 72% 16%, and 8%, respectively. As compared with samples B and C, sample A showed less ash content, and this is considered as an advantage since the lower ash content in the sample is an indication for the higher suitability of the material for thermochemical conversion. Also, the less of moisture content shows the more suitability for thermochemical conversion process since the lower moisture content would affect in higher net calorific value of the material. On the other hand, the increase of volatile contents in the sample would give an indicator of the higher ignitability of the material. Moreover, the higher percentage of fixed carbon would affect positively on the amount of heat released when burning of biomass material. From the previous discussion and from elemental analysis point of view, it is very clear that sample A is more suitable for thermochemical conversion as compared with sample B and C which showed lower quality.

In addition, Table 2 shows a comparison of olive waste samples A, B and C with other different biomass material including Sorghum, Stover and wood. As it can be seen from the Table, sample A showed a superior quality in term of moisture, volatile and fixed carbon as compared with sorghum and Stover since it showed lower percentage of moisture and higher percentage of volatile and fixed carbon. On the other hand, as compared with other materials, sample A showed a higher ash content which indicate a difficulty in ash removing mechanisms. Generally, the material degradation trends showed relatively superior properties for sample A to undergo thermochemical energy conversion.

3.3. Kinetic Model

Heating rate is very important factor which affecting the thermal degradation behavior of biomass materials. Shown in Figure 6-8 are the thermal degradation behavior and derivative mass loss curve (DTG) for heating rate of 5, 10, 30 and 50 k/min of sample A, B and C. As it can be seen from the figures,

increasing of heating rate was affected in shifting of DTG peaks in the direction of higher temperatures. This is due to limitation of heat transfer at higher heating rates where the reaction time will be shorter at higher heating rates [40-42] which would give enough time for the nitrogen to reach an equilibrium conditions with the sample temperature. Thus, in the case of higher heating rates, the amount of heat required for bond cracking reached it value later as compared with the lower heating rates. In addition, for the same heating rates and temperature ranges, sample A showed higher degradation rates as compared with sample B and C. This is because of the lower percentage of cellulose in sample B and C as compared with sample A.

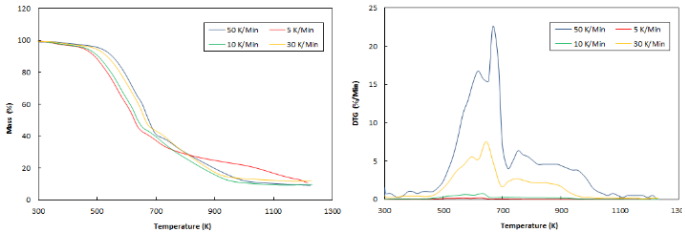

Fig. 6. The thermal degradation behavior and derivative mass loss curve (DTG) of sample A at different heating rate.

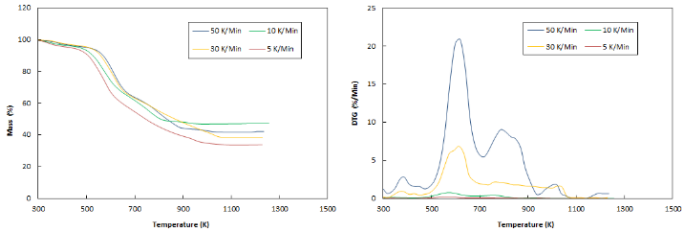

Fig. 7. The thermal degradation behavior and derivative mass loss curve (DTG) of sample B at different heating rate.

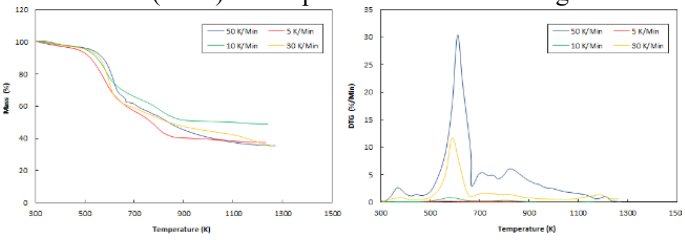

Fig. 8. The thermal degradation behavior and derivative mass loss curve (DTG) of sample C at different heating rate.

Testing of biomass material under different heating rates is a key method for evaluating of kinetic parameters of biomass materials. In this work, the collected data from thermal degradation behavior at different heating rates were used in evaluation of kinetic parameters including calculating of activation energy and finding out of pre-exponential factor for the samples under study. The obtained kinetic parameters were based on Kissinger and the Distributed Activation Energy Model (DAEM).

Kissinger is not is conversional model where the degree of conversion in this model is assumed to be constant for different heating rates. Based on the thermal degradation behavior and derivative mass loss curve (DTG) at different heating rate collected in the previous step, the Kissinger plot for the materials under study were prepared. Shown in Figure 9 are the Kissinger plot of $\ln\left(\frac{\beta}{T_m^2}\right)$ against $\left(\frac{1000}{T_m}\right)$ and the corresponding regression relations lines for sample A, B and C. As it can be seen from the figure, the regression coefficient R2 was varying from 0.9036 for sample A to 0.9427 for sample C. For each sample, the kinetic parameters which include the activation energy and pre-exponential factor were collected from regression line slope and intercept of the linear relationship.

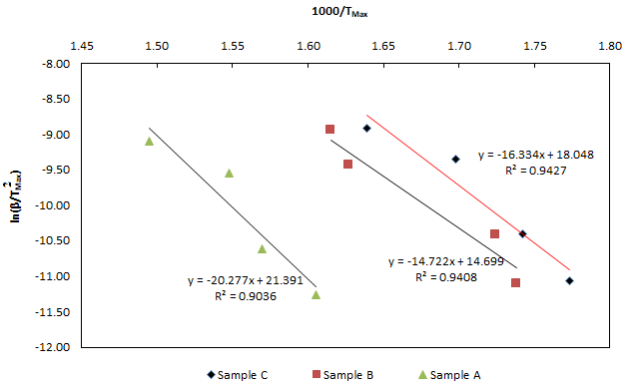

Fig. 9. Kissinger plot for sample A, B and C.

A comparison of the collected activation energy and pre-exponential factor for olive wastes samples including A, B and C based on Kissingar model are shown in Table 4. As it can be seen from the Table, sample A showed relatively higher activation energy as compared with sample B and C which means higher amount of energy needed by sample A inorder to undergo into a thermochemical energy conversion. On the other hand sample A showed a relatively higher pre-eaponential factor as compared with sample B and C. Thus, although the higher value of activation energy needed by sample A in thermochemical energy conversion processes, it relatively reaches this value higher number of times as compared by B and C.

Table 4. A comparison of the activation energy and pre-exponential factor for the samples under study

Sample	Activation Energy (E_a) (kJ/mol)	Pre-exponential factor (A) (Min^{-1})
A	168.50	3.954×10^{13}
B	122.76	3.573×10^{10}
C	135.74	1.125×10^{12}

The activation energy based on the Distributed Activation Energy Model (DAEM) was calculated for different de-volatilization rate. In order to evaluate the kinetic parameters, different de-volatilization ranging from 0.1 to 0.7 were chosen and implemented for the tested samples. This range was used in the current study because thermochemical reactions at the beginning and ending of the de-volatilization process [43]. Shown in Figure 13-15 are the variation of de-volatilization percentage at different heating rates including 5 k/min, 10 K/min, 30 K/min and 50 K/min for the samples under study.

As it can be seen from the figures, similar trends were observed for sample A, B and C. From the figures, higher de-volatilization rate was found to be implemented in the beginning of the de-volatilization process till a temperature of around 800K. Thus, for all tested samples, most of material

de-volatilization process occurs in the temperature range 450 to 800K. After this point, two-stage reduction in the de-volatilization rate was observed. The first stage was in the temperature range of 800 to 950K which is associated with lignin pyrolysis. The second zone was in the temperature greater than 900K which is associated with a relatively lower de-volatilization rate at fixed carbon zone.

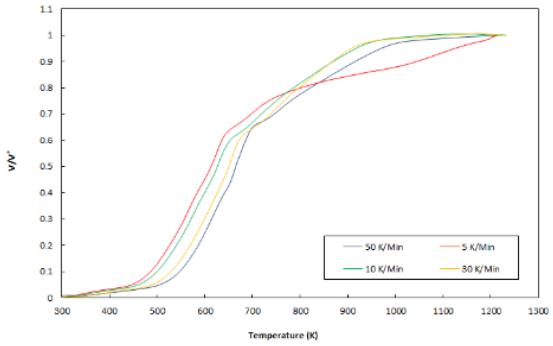

Fig. 10. De-volatilization curves at different heating rate of sample A.

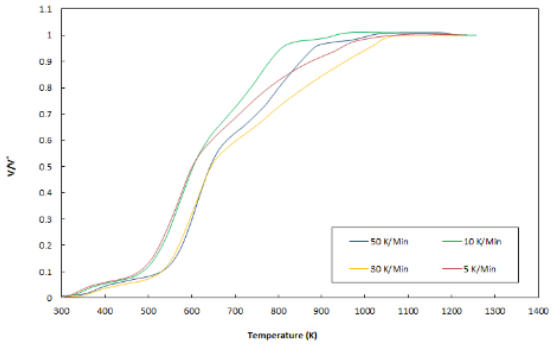

Fig. 11. De-volatilization curves at different heating rate of sample B.

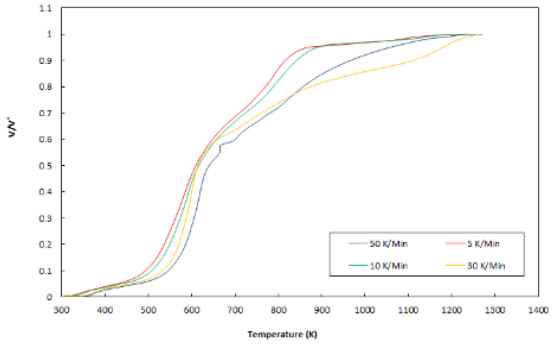

Fig. 12. De-volatilization curves at different heating rate of sample C.

The collected data from de-volatilization curves were used for drawing of the distributed Activation Energy Model (DAEM) curves for selected de-volatilization rates of the samples under study. The plot represents the relation between $\ln \beta_i/T^2$ and$\frac{1000}{T_i}$. Shown in Figure 16-18 are the Distributed Activation Energy Model curve for sample A, B and C, respectively. The comprehensive data collected from the figures which include activation energy along with coefficient of regression (R2) are shown in Table 6. As it can be seen from the coefficient (R2) a linear fitting was obtained for almost de-volatilization. The activation energy (Ea) was calculated from the slope while the pre-exponential factor was calculated from the intercept.

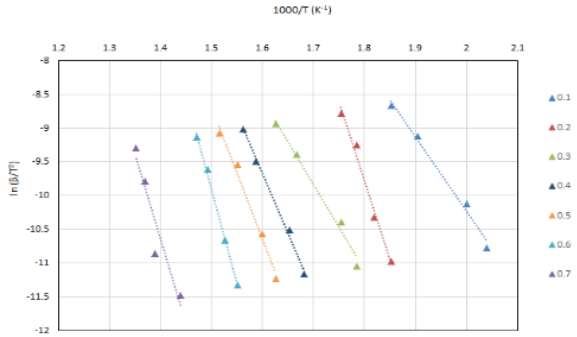

Fig. 13. The activation energy based on (DAEM) model at different de-volatilization rates for sample A.

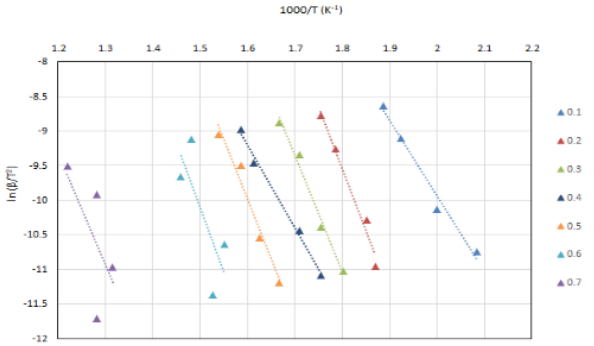

Fig. 14. The activation energy based on (DAEM) model at different de-volatilization rates for sample B.

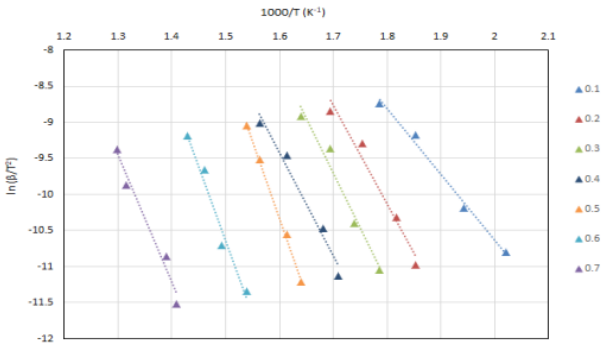

Fig. 15. The activation energy based on (DAEM) model at different de-volatilization rates for sample C.

As it can be seen from Table 5, the obtained activation energy for sample A, B and C was ranging from 91-208 kJ/mol, 90-154 kJ/mol and 75–177 kJ/mol, respectively. For the same de-volatilization rates the activation energy for sample A were found to be higher as compared with sample B and C which were found to be is the same ranges. As it can be seen from the Table, for all tested samples, low activation energy values were observed at very low conversion rates. On the other hand, at the intermediate conversion rates, the activation energy was found to be in its intermediate values. Finally, at high conversion rates, the activation energy increases to a very high value and drop again. The fluctuation in the activation energy values was higher in sample as compared with sample B and C. The observed variation in the

distributed activation energy shows the higher complexity in the degradation process of the material under study. The low values of activation energy may be due to the broken of weak chemical bonds which is associated with a formation of light volatiles. With the progress of de- volatilization process higher activation energies are needed due to covalent chemical bonds. Finally, at the higher conversion rates, the activation energy dropped due to fact the most of bonds were broken. The values of pre-exponential factor for sample A, B and C were found to be in the range of 9.85E+08 to 1.88E+18, 2.23E+08-7.12E+13 and 0.9E+9-2.68E+14.

The average values for activation energy collected from the Distributed Activation Energy Model (DAEM) for sample A, B and C were compared with the corresponding values of Kissinger model. Good agreement was found for activation energy collected based on Kissinger and DAEM models, where the percentage difference for activation energy were found to be 3.05%, 6.0% and 2.1% for A, B and C respectively. The collected results on activation energy and pre-exponential factor were compared with other similar studies. As it can be seen from Table 6, the collected results were in good agreement with the literature results.

Table 5. Activation energy, pre-exponential factor and coefficient of regression (R2) for sample A, B and C

	Sample A			Sample B			Sample C		
$\frac{V}{V^*}$	Activation Energy (kJ/mol)	Relation between $\ln\left(\frac{\beta}{T^2}\right)$vs. 1/T and R^2	A	Activation Energy (kJ/mol)	Relation between $\ln\left(\frac{\beta}{T^2}\right)$vs. 1/T and R^2	A	Activation Energy (kJ/mol)	Relation between $\ln\left(\frac{\beta}{T^2}\right)$vs. 1/T and R^2	A
0.1	91.25	y = -10.981x +11.731 R^2 = 0.9894	7.44E +08	90.16	y = -10.85x +11.76 R^2 = 0.981	7.57E+ 08	75.46	y = -9.081x + 7.5249 R^2 = 0.9919	9169007
0.2	195.69	y = -23.549x +32.617 R^2 = 0.9821	1.88E +18	148.91	y = -17.919x + 22.71 R^2 = 0.9757	7.12E+ 13	113.44	y = -13.651x + 14.44 R^2 = 0.9669	1.39E+10
0.3	106.06	y = -12.763x +11.861 R^2 = 0.9871	9.85E +08	138.22	y = -16.633x +18.917 R^2 = 0.9817	1.49E+ 12	126.82	y = -15.261x + 16.238 R^2 = 0.9638	9.37E+10
0.4	146.40	y = -17.617x + 18.51 R^2 = 0.9942	1.05E +12	99.42	y = -11.964x +9.9419 R^2 = 0.9921	1.35E+ 08	119.08	y = -14.33x + 13.502 R^2 = 0.975	5.71E+09
0.5	162.94	y = -19.608x +20.737 R^2 = 0.987	1.08E +13	145.47	y = -17.505x +18.024 R^2 = 0.9638	6.41E+ 11	177.60	y = -21.372x + 23.861 R^2 = 0.9982	2.68E+14
0.6	233.13	y = -28.055x +32.179 R^2 = 0.9967	1.44E +18	153.97	y = -18.528x +17.685 R^2 = 0.5859	4.84E+ 11	170.83	y = -20.557x + 20.196 R^2 = 0.9711	6.61E+12
0.7	207.99	y = -25.029x +24.366 R^2 = 0.9043	5.21E +14	134.70	y = -16.209x +10.139 R^2 = 0.4238	2.23E+ 08	146.95	y = -17.683x + 13.518 R^2 = 0.9748	7.15E+09
Average	163.35			130.12			132.88		

Table 6. Comparison of activation energy and pre-exponential factor for olive wastes

Sample	Activation Energy (E_a) (kJ/mol)	Pre-exponential factor (A) (Min^{-1})
A (Kissinger)	168.50	3.954×10^{13}
A (Average DAEM)	163.35	7.44E+08-1.88E+18
B (Kissinger)	122.76	3.573×10^{10}
B (Average DAEM)	130.12	2.23E+08-7.12E+13
C (Kissinger)	135.74	1.125×10^{12}
C (Average DAEM)	132.88	9.17E+6-2.68E+14
Olive kernels [27]	130.3	1.18×10^{10}
Olive pomace [27]	149.87	3.32×10^{12}
Olive residue (Ozawa method) [40]	148-207	-
Olive residue (Vyazovkin method) [40]	160-219	-
Olive residue Ozawa–Flynn– Wall method [44]	148-211	-
Poplar wood [45] FWO method	158.58	7.96×10^{13}

4. Conclusion

In this work, the suitability of Saudi Arabian olive wastes for thermochemical energy conversion was studied experimentally by using physical, thermal and elemental investigations. For elemental analysis TGA and CHN analysis were applied. Three samples from different location including one sample from Domat Al-Jandal-KSA and two samples from Elgrayat-KSA were collected and investigated. The lower calorific values for Domat Al-Jandal samples were found to be 24152.5kJ/kg while for Elgrayat samples the value was found to be 12568.5kJ/kg and 13386kJ/kg, respectively. The elemental investigation showed a better quality for Domat Al-Jandal samples as compared with Elgrayat samples where the carbon and hydrogen percentages were found to be 50% and 8%. Based on Kissinger model, the values of activation energy were found to be in the range of 122.77 to 168.50 kJ/mol with a pre-exponential factor ranging from 3.573×10^{10} to 3.954×10^{13}. The collected results on the activation energy was based on Kissinger and DAEM models were within good agreement with the literature, where the percentage difference were found to be in the range of 2.1% to 6.0%. The collected results from this work can be considered as solid base for further studies of olive wastes thermochemical conversion processes such as gasification, pyrolysis and combustion.

References

[1] P. Garcia-Ibanez, M. Sanchez, and A. Cabanillas, "Thermogravimetric analysis of olive-oil residue in air atmosphere," Fuel Processing Technology, vol. 87, pp. 103-107, 2006.

[2] K. Cliffe and S. Patumsawad, "Co-combustion of waste from olive oil production with coal in a fluidised bed," Waste management, vol. 21, pp. 49-53, 2001.

[3] A. Roig, M. L. Cayuela, and M. Sánchez-Monedero, "An overview on olive mill wastes and their valorisation methods," Waste management, vol. 26, pp. 960-969, 2006.

[4] G. Stamatakis, "Energy and geo-environmental applications for olive mill wastes. a review," Hellenic Journal of Geosciences, vol. 45, pp. 269-282, 2010.

[5] H. Mehri, A. Soltane, F. Richene, and K. Mhanna, "Preliminary trials on the reproductive behaviour of five olive cultivars conducted in El-Jouf region (KSA)," American Journal of Plant Physiology, vol. 8, pp. 93-104, 2013.

[6] M. Mridha, A. Al-Qarawi, S. Al-Oud, and F. Al-Barakah, "Status and Need of Research on Growth Improvement of Olive (Olea europaea L.) with Microbial Inoculants in Saudi Arabia," Journal of Pure and Applied Microbiology, Shahjahanabad, vol. 7, pp. 1861-1868, 2013.

[7] M. H. Hemida, A. Ibrahim, R. M. Al-Bahnsawy, and M. R. Al-Shathly, "Influence of environmental factors on olive oil production and quality in the Northern Region of kingdom of Saudi Arabia," J. Am. Sci, vol. 10, pp. 61-66, 2014.

[8] A. Hussein, "Response of Manzanillo olive (Olea europaea, L.) cultivar to irrigation regime and potassium fertigation under tabouk conditions, Saudi Arabia," Journal of Agronomy, 2008.

[9] M. A. Uddin, S. Y. A. Siddiki, S. F. Ahmed, Z. I. Rony, M. Chowdhury, and M. Mofijur, "Estimation of sustainable bioenergy production from olive mill solid waste," Energies, vol. 14, p. 7654, 2021.

[10] A. Demirbas, M. Kabli, R. H. Alamoudi, W. Ahmad, and A. Basahel, "Renewable energy resource facilities in the Kingdom of Saudi Arabia: Prospects, social and political challenges," Energy Sources, Part B: Economics, Planning, and Policy, vol. 12, pp. 8-16, 2017.

[11] T. Alkhamis and M. Kablan, "Olive cake as an energy source and catalyst for oil shale production of energy and its impact on the environment," Energy Conversion and Management, vol. 40, pp. 1863-1870, 1999.

[12] M. Guida, H. Bouaik, A. Tabal, A. Hannioui, A. Solhy, A. Barakat, et al., "Thermochemical treatment of olive mill solid waste and olive mill wastewater: Pyrolysis kinetics," Journal of Thermal Analysis and Calorimetry, vol. 123, pp. 1657-1666, 2016.

[13] R. Volpe, A. Messineo, M. Millan, M. Volpe, and R. Kandiyoti, "Assessment of olive wastes as energy source: pyrolysis, torrefaction and the key role of H loss in thermal breakdown," Energy, vol. 82, pp. 119-127, 2015.

[14] C. Guizani, K. Haddad, M. Jeguirim, B. Colin, and L. Limousy, "Combustion characteristics and kinetics of torrefied olive pomace," Energy, vol. 107, pp. 453-463, 2016.

[15] P. McKendry, "Energy production from biomass (part 2): conversion technologies," Bioresource technology, vol. 83, pp. 47-54, 2002.

[16] J. Wang, L. Wen, Y. Chen, and H. Han, "Study on the combustion characteristics and kinetics of biomass and coal char blended fuels," in 2018 7th International Conference on Renewable Energy Research and Applications (ICRERA), 2018, pp. 576-581.

[17] F. Resende, V. Silva, M. Mendonça, A. Barbosa, P. Brito, J. Azevedo, et al., "Using biomass gasification for small scale power generation systems: specifications of the conceptual framework," in 2019 8th International Conference on Renewable Energy Research and Applications (ICRERA), 2019, pp. 439-444.

[18] C. M. Sastre, Y. G. Arechavala, and A. M. S. Montes, "Evaluation of the environmental sustainability of the use of straw for electricity production," in 2013 International Conference on Renewable Energy Research and Applications (ICRERA), 2013, pp. 722-727.

[19] S. Yılmaz and H. Selim, "A review on the methods for biomass to energy conversion systems design," Renewable and Sustainable Energy Reviews, vol. 25, pp. 420-430, 2013.

[20] S. C. Capareda, "Biomass energy conversion," in Sustainable growth and applications in renewable energy sources, ed: IntechOpen, 2011.

[21] B. Khalida, Z. Mohamed, S. Belaid, H. O. Samir, K. Sobhi, and S. Midane, "Prediction of higher heating value HHV of date palm biomass fuel using artificial intelligence method," in 2019 8th International Conference on Renewable Energy Research and Applications (ICRERA), 2019, pp. 59-62.

[22] E. Christoforou and P. A. Fokaides, "A review of olive mill solid wastes to energy utilization techniques," Waste Management, vol. 49, pp. 346-363, 2016.

[23] P. McKendry, "Energy production from biomass (part 3): gasification technologies," Bioresource technology, vol. 83, pp. 55-63, 2002.

[24] I. Carlucci, G. Mutani, and M. Martino, "Assessment of potential energy producible from agricultural biomass in the municipalities of the Novara plain," in 2015 International Conference on Renewable Energy Research and Applications (ICRERA), 2015, pp. 1394-1398.

[25] F. Göğüş and M. Maskan, "Air drying characteristics of solid waste (pomace) of olive oil processing," Journal of Food Engineering, vol. 72, pp. 378-382, 2006.

[26] T. Miranda, J. Arranz, I. Montero, S. Román, C. Rojas, and S. Nogales, "Characterization and combustion of olive pomace and forest residue pellets," Fuel Processing Technology, vol. 103, pp. 91-96, 2012.

[27] K. Al bkoor Alrawashdeh, K. Slopiecka, A. A. Alshorman, P. Bartocci, and F. Fantozzi, "Pyrolytic degradation of olive waste residue (OWR) by TGA: thermal decomposition behavior and kinetic study," Journal of Energy and Power Engineering, vol. 11, pp. 497-510, 2017.

[28] J. J. Manyà, F. X. Roca, and J. F. Perales, "TGA study examining the effect of pressure and peak temperature on biochar yield during pyrolysis of two-phase olive mill waste," Journal of analytical and applied pyrolysis, vol. 103, pp. 86-95, 2013.

[29] A. Soria-Verdugo, E. Goos, and N. García-Hernando, "Effect of the number of TGA curves employed on the biomass pyrolysis kinetics results obtained using the Distributed Activation Energy Model," Fuel Processing Technology, vol. 134, pp. 360-371, 2015.

[30] J. Jauhiainen, J. A. Conesa, R. Font, and I. Martın-Gullón, "Kinetics of the pyrolysis and combustion of olive oil solid waste," Journal of Analytical and Applied Pyrolysis, vol. 72, pp. 9-15, 2004.

[31] H. E. Kissinger, "Variation of peak temperature with heating rate in differential thermal analysis," Journal of research of the National Bureau of Standards, vol. 57, pp. 217-221, 1956.

[32] V. Vand, "A theory of the irreversible electrical resistance changes of metallic films evaporated in vacuum," Proceedings of the Physical Society (1926-1948), vol. 55, p. 222, 1943.

[33] K. Miura and T. Maki, "A simple method for estimating f (E) and k 0 (E) in the distributed activation energy model," Energy & Fuels, vol. 12, pp. 864-869, 1998.

[34] K. Miura, "A new and simple method to estimate f (E) and k0 (E) in the distributed activation energy model from three sets of experimental data," Energy & Fuels, vol. 9, pp. 302-307, 1995.

[35] S. Abdullah, S. Yusup, M. M. Ahmad, A. Ramli, and L. Ismail, "Thermogravimetry study on pyrolysis of various lignocellulosic biomass for potential hydrogen production," in Proceedings of World Academy of Science, Engineering and Technology, 2010, pp. 129-133.

[36] Y. Demirel, "Energy and energy types," in Energy, ed: Springer, 2012, pp. 27-70.

[37] A. Korotkikh, K. V. Slyusarskiy, K. B. Larionov, and V. I. Osipov, "Comparison of coal reactivityduring conversion into different oxidizing medium," in Journal of Physics: Conference Series, 2016, pp. 052005.1-5.

[38] C. Di Blasi, "Modeling chemical and physical processes of wood and biomass pyrolysis," Progress in energy and combustion science, vol. 34, pp. 47-90, 2008.

[39] P. McKendry, "Energy production from biomass (part 1): overview of biomass," Bioresource technology, vol. 83, pp. 37-46, 2002.

[40] A. Ounas, A. Aboulkas, A. Bacaoui, and A. Yaacoubi, "Pyrolysis of olive residue and sugar cane bagasse: non-isothermal thermogravimetric kinetic analysis," Bioresource technology, vol. 102, pp. 11234-11238, 2011.

[41] C. Gai, Y. Zhang, W.-T. Chen, P. Zhang, and Y. Dong, "Thermogravimetric and kinetic analysis of thermal decomposition characteristics of low-lipid microalgae," Bioresource technology, vol. 150, pp. 139-148, 2013.

[42] T. Mani, P. Murugan, J. Abedi, and N. Mahinpey, "Pyrolysis of wheat straw in a thermogravimetric analyzer: effect of particle size and heating rate on devolatilization and estimation of global kinetics," Chemical engineering research and design, vol. 88, pp. 952-958, 2010.

[43] N. Koga and J. Criado, "The influence of mass transfer phenomena on the kinetic analysis for the thermal decomposition of calcium carbonate by constant rate thermal analysis (CRTA) under vacuum," International journal of chemical kinetics, vol. 30, pp. 737-744, 1998.

[44] N. Y. Harun, M. T. Afzal, and N. Shamsudin, "Reactivity studies of sludge and biomass combustion," International Journal of Engineering (IJE), vol. 3, pp. 413-426, 2009.

[45] K. Slopiecka, P. Bartocci, and F. Fantozzi, "Thermogravimetric analysis and kinetic study of poplar wood pyrolysis," Applied Energy, vol. 97, pp. 491-497, 2012.